Aluminium(III) porphyrin based dimers and trimers: synthesis, spectroscopy and photochemistry

P. Prashanth Kumar and Bhaskar G. Maiya*

Shool of Chemistry, University of Hyderabad, Hyderabad 500 046, India.
E-mail: bgmsc@uohyd.ernet.in; Fax: +091 (0)40 2301 2460

Received (in Montpellier, France) 27th August 2002, Accepted 5th November 2002
First published as an Advance Article on the web 14th February 2003

The well-known oxophilicity of aluminum(III) ion and the well-defined redox and photochemical properties of aluminum(III) porphyrins have been exploited to synthesize the functionally active, 'axial-bonding'-type free base–aluminum(III) porphyrin dimer (H_2–Al) and free base–[aluminum(III) porphyrin]$_2$ trimer (H_2–Al_2), as well as the corresponding copper(II) (Cu–Al, Cu–Al_2) and zinc(II) (Zn–Al, Zn–Al_2) derivatives. These dimeric and trimeric species have been fully characterized by mass (FAB), UV/VIS, proton nuclear magnetic resonance (1D and ^{1}H-^{1}H COSY) and electron spin resonance spectroscopies and also by the differential pulse voltammetric method. Comparison of their spectroscopic and electrochemical data with those of the corresponding monomeric porphyrins reveals that there is no apparent ring-to-ring interactions in these 'vertically' linked dimers and trimers. The fluorescence quantum yields and singlet state life times were found to be lower for H_2–Al and H_2–Al_2 in comparison with those of the monomeric chromophores. Electronic energy transfer from the aluminum(III) porphyrin to the free base subunit is detected in both H_2–Al and H_2–Al_2. Finally, a comparison is made between the presently reported aluminum(III) porphyrin based arrays and the previously reported analogous arrays based on tin(IV), germanium(IV) and phosphorous(V) porphyrins with regard to their architectural features, spectroscopic properties and photochemical activities.

Currently, a great variety of molecular arrays based on metalloporphyrin species are being investigated for their utility in research areas such as biomimetic photosynthesis, molecular electronics/photonics, molecular catalysis, *etc.*[1–12] In contrast, less attention seems to have been paid towards analogous species based on the main group/metalloid ion containing porphyrins. Only a few phosphorus(V) , tin(IV), germanium(IV) and gallium(III) porphyrin based 'axial-bonding' type cyclic/noncyclic oligomers have been reported so far, with the majority of them having been constructed by utilizing the oxophilicity of the central metalloid ion.[13–21] Aluminum(III) ion is also oxophilic[22] but, to the best of our knowledge, functionally active Al(III) porphyrin based molecular arrays have never been synthesized. On the other hand, monomeric Al(III) porphyrins are known to possess rich redox and photochemical activities and, in addition, have received attention as catalysts for various organic transformations.[23–27] We sought to harness the well-known strength of the Al–O bond and the well-defined redox and photochemical properties of Al(III) porphyrins to build functionally active molecular arrays. Results of our efforts in this direction are discussed in this paper, which reports the synthesis, characterization and photochemical properties of three dimeric (H_2–Al, Cu–Al and Zn–Al) and three trimeric (H_2–Al_2, Cu–Al_2 and Zn–Al_2) 'axial-bonding' type systems based on the Al(III) porphyrin scaffold, Fig. 1.

Experimental

The chemicals and solvents utilized in this study were purchased from either Aldrich Chemical Co. (USA) or E. Merck (India). The solvents utilized for spectroscopic and electrochemical experiments were further purified using standard procedures.[28]

Syntheses

The precursor porphyrins, *viz.* 5,10,15,20-tetra(4-methyphenyl)porphyrin (H_2L^1),[29] 5-(4-hydroxyphenyl)-10,15,20-tri(4-methyphenyl)porphyrin (H_2L^2)[30] and 5,15-bis(4-hyroxyphenyl)-10,20-bis(4-methyphenyl)porphyrin (H_2L^3)[31] were synthesized by established methods. Al(III) porphyrin derivatives [(L^1)Al^{III}Cl] and [(L^1)Al^{III}OH] were also prepared and purified according to the reported procedures.[32] Procedures for the synthesis of the new dimeric and trimeric porphyrins are detailed below.

H_2–Al. A solution containing 0.10 g (0.14 mmol) of [(L^1)Al^{III}OH] and 0.28 g (0.42 mmol) of H_2L^2 in 30 ml of dry C_6H_6 was refluxed under a nitrogen atmosphere for 12 h. The solvent was removed under vacuum and the crude product was chromatographed on alumina (neutral, activity 1). Elution with $CHCl_3$–hexane (60:40, V/V) separated the desired (aryloxo) aluminium(III) derivative as a purple-coloured band. The solvents were removed under reduced pressure and the resulting solid was recrystallised twice from CH_2Cl_2–hexane to give the pure product. Yield = 0.11 g (62%). FAB-MS: $(M+H)^+$, 1368; $(M-C_{47}H_{35}N_4O)^+$, 696; $(M-C_{48}H_{36}N_4Al)^+$, 672.

H_2–Al_2. This trimer was prepared by refluxing a dry C_6H_6 solution (50 ml) containing 0.10 g (0.14 mmol) of H_2L^3 and 0.57 g (0.84 mmol) of [(L^1)Al^{III}OH] under a nitrogen atmosphere for 12 h. The work-up of the reaction mixture as described above for H_2–Al furnished 0.19 g (65%) of the trimer in pure form. FAB-MS: $(M)^+$, 2064; $(M-C_{48}H_{36}N_4Al)^+$, 1369; $(C_{48}H_{36}N_4Al)^+$, 696; $[M-2\times(C_{48}H_{36}N_4Al)]^+$/$C_{46}H_{32}N_4O_2$, 672.

Metallo-metalloid dimers and trimers. Dimers Cu–Al and Zn–Al and trimers Cu–Al_2 and Zn–Al_2 were prepared by

DOI: 10.1039/b208339f

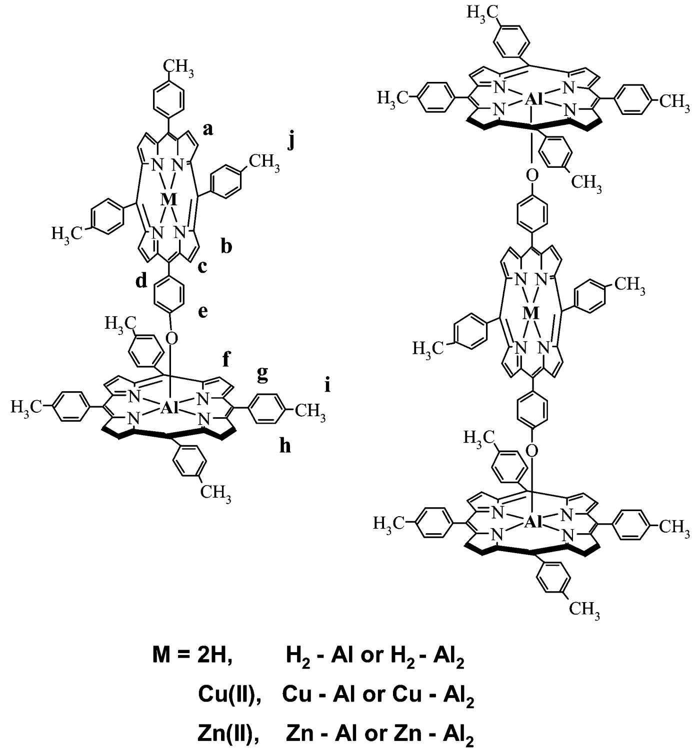

Fig. 1 "Axial-bonding" type hybrid dimers and trimers based on the Al(III) porphyrin scaffold.

metallating H_2–Al or H_2–Al_2 with the corresponding metal(II) acetates by the standard methods.[33] Typically, 0.1 g of H_2–Al/H_2–Al_2 and 0.1 g of either copper(II) acetate or zinc(II) acetate were stirred in a $CHCl_3$–CH_3OH mixture for 0.5–1 h. The solvents were evaporated and the residue was washed with water and dried. Purification by column chromatography ($CHCl_3$; alumina, activity 1) furnished the pure product in each case. Yields ranged typically from 70 to 80%.

Methods

Care was taken to avoid the entry of direct, ambient light into the samples in all the spectroscopic and electrochemical experiments described below. Unless otherwise specified, all the experiments were carried out at 293 ± 3 K.

The UV/VIS spectra were recorded with a Shimadzu Model UV-3101PC UV/VIS spectrophotometer on 1×10^{-6} M (Soret band)–5×10^{-5} M (Q bands) solutions of the porphyrins. Steady-state fluorescence spectra (uncorrected) were recorded using a Spex Model Fluoromax–3 spectrofluorimeter on $\cong 5 \times 10^{-7}$ M (O.D. at $\lambda_{ex} < 0.2$) solutions. The emitted quanta were detected at right angle to the incident beam. The fluorescence quantum yields (ϕ) were estimated by integrating the fluorescence bands and by using either 5,10,15,20-tetraphenylporphyrin (H_2TPP) ($\phi = 0.13$ in CH_2Cl_2) or 5,10,15,20-tetraphenylporphyrinato zinc(II) ($[(TPP)Zn^{II}]$) ($\phi = 0.036$ in CH_2Cl_2) as the standard.[34,35] Refractive index corrections have been incorporated while reporting the fluorescence data in various solvents. Dilute solutions ($\sim 10^{-7}$ M) of the fluorophores were utilized for the excitation spectral measurements. Corrections to the instrument response (up to 650 nm) and procedures for the spectral normalization employed during the estimations of the excitation energy transfer efficiencies are essentially similar to those described in our previous studies.[36–38] Fluorescence life times were measured by the time-correlated single photon counting (TCSPC) method, as described previously.[39,40] Briefly, the samples were excited by 4 ps laser (Nd/YAG pumped Rhodamine 6G dye laser) pulses at a repletion rate of 800 kHz. The fluorescence was detected at the magic angle (54.7°) with respect to polarization of the incident beam by a microchannel plate photomultiplier (MCP PMT, R2809). The count rate employed was typically 2×10^4 s^{-1}. The excitation wavelength was fixed at 575 nm and the fluorescence was collected at either 720 nm (free base porphyrin) or 600 nm [Al(III) porphyrin]. Deconvolution of the data was carried out by the method of iterative reconvolution of the instrument response function and the assumed decay function. The goodness-of-fit of the experimental data to the assumed decay function was judged by standard statistical tests (*i.e.*, random distribution of weighted residuals, the autocorrelation function and the values of reduced χ^2).

FAB mass spectra were recorded with a JEOL SX 102/DA-6000 mass spectrometer/data system. ^1H NMR spectra were recorded with either a Bruker NR-200 AF-FT or Bruker DRX-500 spectrometer using $CDCl_3$ as the solvent and tetramethylsilane (TMS) as an internal standard. ESR spectra were run on a JEOL JES-FA200 X-band ESR spectrometer for the copper(II) systems in toluene at 100 ± 3 K. Diphenyl picryl hydrazide (DPPH) was used as the g marker. Cyclic and differential pulse voltammetric experiments (CH_2Cl_2, 0.1 M tetrabutylammonium perchlorate, TBAP) were performed on a CH Instruments model CHI 620A electrochemical analyzer as detailed in our previous studies (working and auxillary electrodes: Pt; reference electrode: SCE).[36–38,41–45] The Fc^+/Fc (Fc = ferrocene) couple was used to calibrate the redox potential values.

Results and discussion

Design and synthesis

Relying largely on the oxophilicity of the Al(III) ion, synthesis of H_2–Al and H_2–Al_2 and also their Cu(II) and Zn(II) derivatives has been accomplished here, in good to moderate yields, following a step-wise protocol that we had adopted earlier for the synthesis of P(V), Sn(IV) and Ge(IV) porphyrin trimers.[41–43]

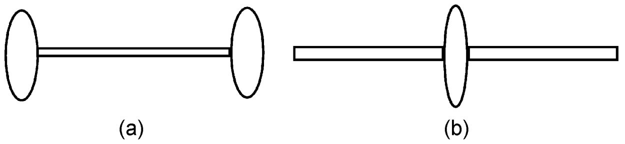

Fig. 2 Topological features of the trimeric species derived from (a) Al(III) porphyrin and (b) P(V)/Sn(IV)/Ge(IV) porphyrins.

There, however, exist important differences between these old and new arrays with regard to their design and architectural features. These are: (i) reaction of the hydroxy Al(III) porphyrin [(L^1)Al^{III}OH] with excess H_2L^2 provides easy access to a dimeric porphyrin, whereas this was not the case with the P(V), Sn(IV) and Ge(IV) porphyrins. Having been endowed with two axial hydroxy/chloro groups, the latter metalloid porphyrins reacted with excess H_2L^2, invariably yielding the trimeric species.[41,42] (ii) On the other hand, synthesis of trimer H_2–Al_2 has been achieved here by the reaction of [(L^1)Al^{III}OH] with the meso *trans*-dihydroxy porphyrin H_2L^3. Thus, trimers derived from the Al(III) porphyrin contain two metalloid porphyrins, whereas the other trimers posses only one metalloid porphyrin in their respective architectures. (iii) Consequently, the gross topological features of the trimeric species derived from the Al(III) porphyrin are also quite different from those of the P(V)/Sn(IV)/Ge(IV) porphyrin species, as schematically illustrated in Fig. 2.

The above considerations permit us to elucidate the role of structural features on the spectroscopic properties and photochemical functions of the Al(III) porphyrin based arrays on the one hand, and of the P(V), Sn(IV) and Ge(IV) porphyrin based arrays on the other. In addition, the availability of both H_2–Al and H_2–Al_2 [and also the corresponding copper(II) and zinc(II) derivatives] provides an opportunity to compare and contrast properties of the dimeric and trimeric porphyrins that belong to the same 'class'. We have attempted to address these issues while presenting the spectroscopic, redox and photochemical data of these new arrays, as discussed below.

Spectroscopic characterization

The mass (FAB) spectra of both H_2–Al and H_2–Al_2 (see Experimental) showed a low intensity peak ascribable to the parent M^+ ion in each case. However, the peaks due to those fragments obtained upon elimination of the axial free base porphyrin(s) were found to be intense as is the case with the axial-bonding type, penta- and hexa-coordinated metalloid porphyrins previously investigated by several workers, including ourselves.[41–45]

The ^{1}H NMR spectral data of the diamagnetic dimers and trimers along with those of the individual unlinked monomers are summarized in Table 1 and the spectra of H_2L^2, [(L^1)Al^{III}OH] and H_2–Al are compared in Fig. 3. As seen from this figure and the data given in Table 1, the resonance positions of the protons on the basal Al(III) porphyrin components (protons f, g, h and i; see Fig. 1 for proton assignments) of H_2–Al and H_2–Al_2 are more or less similar to those of [(L^1)Al^{III}OH] {or [(L^1)Al^{III}Cl]}. On the other hand, the resonance positions and also the splitting patterns of the protons on their axial free base porphyrins are quite different from those of H_2L^2 or H_2L^3 as a result of the ring current effect exerted by the basal Al(III) porphyrin(s).[46] As such, the ortho and meta (with respect to the axial 'oxo' group) protons of the bound porphyrin-aryloxo ligand in H_2–Al are shielded and resonate at 2.76 (d, 2H, protons e) and 6.63 (d, 2H, protons d) ppm, respectively (identified by ^{1}H-^{1}H COSY experiment). The $\Delta\delta$ values [*i.e.*, $\delta(H_2L^2) - \delta(H_2\text{–Al})$] for these protons are 4.41 and 1.47 ppm, respectively. The corresponding resonances for H_2–Al_2 are seen to be further shifted upfield (compared to the corresponding protons on H_2L^3) and resonate at 2.75 (d, 2H, protons e) and 6.57 (d, 2H, protons d) ppm with $\Delta\delta$ values [*i.e.*, $\delta(H_2L^3) - \delta(H_2\text{–}Al_2)$] of 4.50 and 1.53 ppm, respectively (Table 1). The higher $\Delta\delta$ values observed for H_2–Al_2 in comparison with H_2–Al can be traced to the unique topology of this trimer [see Fig. 2(a)]. The ortho and meta protons present on the two trans aryloxo groups of H_2–Al_2 are expected to experience the shielding effect by both the axial Al(III) porphyrins [albeit of differing magnitudes, with the 'proximal' Al(III) porphyrin having a stronger effect than the 'distal' one for each set of 'trans' ortho and meta protons]. On the other hand, corresponding protons of the dimer [and also those on the P(V), Sn(IV) and Ge(IV) porphyrin based trimers shown in Fig. 2(b)] are influenced by the shielding effect of only one basal porphyrin.

Another consequence of the topological differences between the dimeric and the trimeric species concerns the ^{1}H NMR resonance pattern and extent of shielding observed for the pyrrole-β protons of their free base components. The pyrrole-β signals of the axial free base porphyrin of H_2–Al are seen to be shifted to the upfield region (compared to those on H_2L^2) and also split into a singlet at δ 8.71 (4H, protons a) and a pair of doublets at δ 8.52 (2H, protons b) and 8.12 (2H, protons c), respectively (see Figs. 1 and 3). This result is similar to that reported for the P(V), Sn(IV) and Ge(IV) porphyrin based trimers and can be accounted for by invoking the porphyrin ring current model.[46] The $\Delta\delta$ values for protons a, b and c of H_2–Al are 0.15, 0.34, 0.74 ppm in that order. On the other hand, higher $\Delta\delta$ values for protons b and c (0.41 and 0.81 ppm,

Table 1 ^{1}H NMR data of H_2–Al, Zn–Al, H_2–Al_2 and Zn–Al_2[a]

	δ					
Array	β-pyrrole (Al) (proton f)	β-pyrrole (axial H_2/Zn)[b] (protons c, b, a)	Bridging aryloxo[b] (protons d, e)	–NH[b]	*meso*-Tolyl (protons g, h)	–CH_3 (protons i, j)
H_2–Al	9.10 (s, 8H)	8.12 (d, 2H) [0.74]; 8.52 (d, 2H) [0.34] $J = 4.9$; 8.71 (s, 4H) [0.15]	6.63 (d, 2H) [1.47]; 2.76 (d, 2H) [4.41] $J = 7.7$	−2.86 (s, 2H) [0.10]	8.05 (d, 8H); 7.97 (m, 6H); 7.47 (m, 14H)	2.58 (s, 9H); 2.62 (s, 12H)
Zn–Al	9.11 (s, 8H)	8.31 (d, 2H) [0.59]; 8.70 (d, 2H) [0.20] $J = 4.7$; 8.84 (s, 4H) [0.06]	6.65 (d, 2H) [1.45]; 2.84 (d, 2H) [4.34] $J = 8.0$	—	8.17 (d, 8H); 8.08 (m, 6H); 7.46 (m, 14H)	2.59 (s, 9H); 2.63 (s, 12H)
H_2–Al_2	9.16 (s, 16H)	8.05 (d, 4H) [0.81]; 8.45 (d, 4H) [0.41] $J = 4.3$	6.57 (d, 4H) [1.53]; 2.75 (d, 4H) [4.50] $J = 7.7$	−2.99 (s, 2H) [0.24]	8.03 (d, 16H); 8.00 (m, 4H); 7.50 (m, 20H)	2.65 (s, 6H); 2.69 (s, 24H)
Zn–Al_2	9.17 (s, 16H)	8.30 (d, 4H) [0.60]; 8.70 (d, 4H) [0.21] $J = 4.9$	6.65 (d, 4H) [1.46]; 2.76 (d, 4H) [4.42] $J = 7.7$	—	8.25 (d, 16H); 8.16 (m, 4H); 7.53 (m, 20H)	2.66 (s, 6H); 2.70 (s, 24H)

[a] Spectra were run in $CDCl_3$ with TMS. Error limits: δ, ±0.01 ppm, *J*, ±1 Hz. [b] Numbers within the square brackets refer to the $\Delta\delta$ values (*i.e.*, $\delta_{\text{monomer}} - \delta_{\text{array}}$; see text for details).

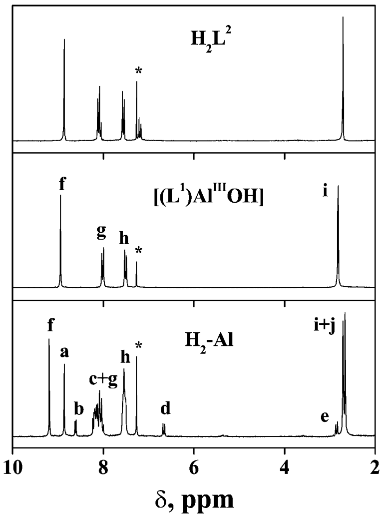

Fig. 3 ^1H NMR spectrum of H_2L^2, $[(L^1)Al^{III}OH]$ and H_2–Al in $CDCl_3$.

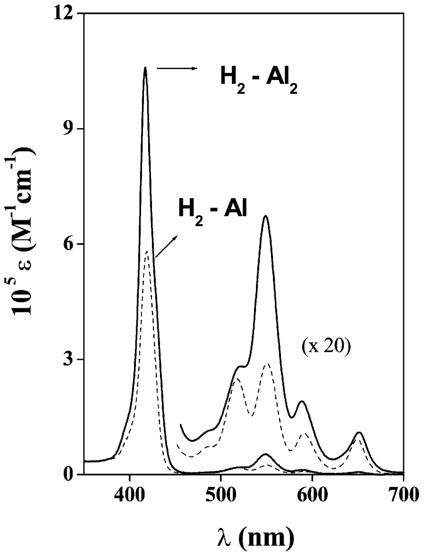

Fig. 4 UV/VIS spectra of H_2–Al and H_2–Al_2 in CH_2Cl_2.

respectively) are noticed for the trimer H_2–Al_2. There is an obvious absence of protons of type a in this trimer due to its architectural symmetry; a symmetric resonance pattern (AB) is observed for protons b and c.

The UV/VIS data of the new dimers, trimers and the those of the corresponding monomeric species, H_2L^1, L^1Cu, L^1Zn, H_2L^2, H_2L^3, $[(L^1)Al^{III}Cl]$ and $[(L^1)Al^{III}OH]$, are summarized in Table 2. Dilute solutions containing 1:1 or 1:2 molar equivalents of H_2L^2:$[(L^1)Al^{III}OH]$ or H_2L^3:$[(L^1)Al^{III}OH]$ generate UV/VIS spectra that are close to the sum of the individual spectra in each case and compare very favourably to the spectra of H_2–Al or H_2–Al_2, with only very minor shifts in the wavelengths of the maximum absorption (λ_{max}) values. It was noticed, however, that the corresponding molar extinction coefficient values (ε) of the trimeric species are generally higher than those of the dimers, as illustrated in Fig. 4 for H_2–Al and H_2–Al_2. Similarly, in the differential pulse voltammetric experiments, the current values corresponding to the oxidation and reduction peaks of the Al(III) porphyrin components of the trimeric systems are higher than those of the corresponding dimeric species. However, the redox potential values of H_2–Al or H_2–Al_2 are close to those of the corresponding monomeric free base and Al(III) porphyrins, Table 3. Analogous results have been obtained for dimers Cu–Al and Zn–Al and trimers Cu–Al_2 and Zn–Al_2 in that the UV/VIS and redox data of these species are similar to the corresponding data obtained for the physical mixtures of the monomeric porphyrins constituting them (see Tables 2 and 3). The ESR spectral parameters of Cu–Al and Cu–Al_2 are also indistinguishable from those of $[(L^1)Cu^{II}]$ {$g_{\parallel}$, $g_{\perp}$ and $A_{\parallel}^{Cu}$, $A_{\perp}^{Cu}$, $A_{\parallel}^{N}$ and $A_{\perp}^{N}$ ($\times 10^4$ cm^{-1}) values are: Cu–Al: 2.172, 2.030, 211, 33.4, 15.7 and 16.7; Cu–Al_2: 2.164, 2.037, 212, 33.8, 15.1 and 16.9; $[(L^1)Cu^{II}]$: 2.187, 2.032, 214, 33.2, 15.0, 16.6}.

Overall, the spectroscopic and electrochemical results obtained for these new 'axial-bonding' type systems are reminiscent of those obtained for the several P(V), Sn(IV) and Ge(IV) based porphyrin trimeric, hexameric and nonameric arrays reported by us earlier.[41–44] These results are also consistent with the fact that there is minimal perturbation of the electronic structures of the individual macrocyclic π systems in H_2–Al and H_2–Al_2 and their Cu(II) and Zn(II) derivatives. Specifically, there exists no indication of the presence of exciton coupling between the porphyrin rings.

Table 2 UV/VIS data of the dimers, trimers and their constituent monomeric porphyrins[a]

Compound	Soret band i_{max}/ nm (log ε)	Q-bands λ_{max}/ nm (log ε)
H_2L^1	419 (5.58)	516 (3.95); 552 (3.72); 592 (3.47); 648 (3.44)
H_2L^2	420 (5.57)	516 (4.04); 552 (3.89); 592 (3.63); 648 (3.59)
H_2L^3	420 (5.48)	517 (3.83); 552 (3.65); 592 (3.36); 648 (3.34)
$[(L^1)Al^{III}OH]$	418 (5.62)	548 (4.09); 587 (3.44)
L^1Cu	416 (5.72)	539 (4.29)
L^1Zn	420 (5.48)	548 (4.38); 587 (3.75)
H_2–Al	419 (5.76)	517 (4.09); 551 (4.16); 591 (3.73); 649 (3.66)
Cu–Al	417 (5.93)	543 (4.75); 580 (4.01)
Zn–Al	419 (5.58)	549 (4.30); 600 (3.88)
H_2–Al_2	417 (6.28)	522 (4.57); 549 (4.97); 588 (4.41); 652 (4.03)
Cu–Al_2	417 (5.75)	549 (4.51); 600 (4.09)
Zn–Al_2	417 (5.72)	548 (4.34); 588 (3.70)

[a] Spectra were measured in CH_2Cl_2. Error limits: λ_{max}, ±1 nm, log ε, ±7%.

Table 3 Redox potential data of the dimers, trimers and the corresponding monomers in CH_2Cl_2 with 0.1 M TBAP[a]

	Potential/V *vs.* SCE	
Compound	Oxidation	Reduction
H_2L^1	1.13, 1.37	−1.03, −1.35
L^1Cu	1.19, 1.48	−1.08, −1.50
L^1Zn	0.90, 1.21	−1.37, −1.54
$[(L^1)Al^{III}$ OH]	1.07, 1.30, 1.62	−1.01, −1.40
$[(L^1)Al^{III}$ (O-p-Cre)][b]	1.14, 1.25	−1.07, −1.30
H_2–Al	1.01, 1.10, 1.31, 1.49	−1.06, −1.42
Cu–Al	1.08, 1.37, 1.58	−1.19, −1.41
Zn–Al	0.88, 1.07, 1.32, 1.46	−1.22, −1.43, −1.61
H_2–Al_2	0.90, 1.06, 1.29, 1.65	−1.13, −1.40
Cu–Al_2	1.16, 1.41, 1.57	−1.23, −1.52
Zn–Al_2	0.81, 1.03, 1.31, 1.45	−0.96, −1.21, −1.50

[a] Error limits: $E_{1/2}$, ±0.03 V. [b] Data on $[(L^1)Al^{III}$ (O-p-Cre)], where O-p-Cre is the axially ligated *p*-cresol group, is given for comparison.

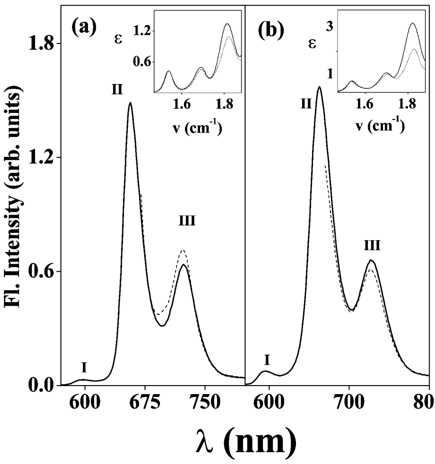

Fig. 5 Fluorescence spectra of (a) H_2–Al and (b) H_2–Al_2 in toluene: (—) λ_{ex} = 550 nm and (---) λ_{ex} = 650 nm. The inset in each figure shows the overlap of the excitation (---) and absorption (—) spectra in toluene (λ_{em} = 720 nm). Numbers appearing on both the ε and ν axes have been divided by 10^4. The excitation spectra were corrected for the instrument response function and were normalized with respect to the absorption spectra between 14 727–16 000 cm^{-1}.

Fluorescence properties

Steady-state fluorescence spectra of H_2–Al and H_2–Al_2 measured in toluene are illustrated in Fig. 5. Analogous spectra were obtained in CH_2Cl_2, CH_3CN and DMF. As seen in Fig. 5, while excitation at 550 nm [where both free base and Al(III) porphyrins absorb; see Fig. 4 and Table 2] results in the appearance of fluorescence bands due to free base (bands II and III) and Al(III) porphyrin (bands I and II) components, while the spectrum with 650 nm excitation (where only free base porphyrin absorbs; see Fig. 4) shows a band exclusively due to the free base component in the ~720 nm (band III) region. It was found that while the fluorescence band maxima of Al(III) and free base components are quite close to those of H_2L^1 or $[(L^1)Al^{III}OH]$, respectively, the fluorescence quantum yields of both components are quenched in comparison with the reference compounds mentioned above. Based on the quantum yield data, % quenching efficiencies %Q(Al) (from data obtained upon excitation at 550 nm and emission monitored in the band I region) and %$Q(H_2)$ (from data obtained upon excitation at 650 nm and emission monitored in the band III region) were calculated and are summarized in Table 4. Inspection of the data presented in Table 4 reveals that the %Q(Al) values are invariably higher than the %$Q(H_2)$ values for both H_2–Al and H_2–Al_2 in each solvent. The time-resolved fluorescence data also suggest the same as discussed below.

While emission decays of H_2L^1 and the free base components of H_2–Al and H_2–Al_2 were monitored at 720 nm, those of $[(L^1)Al^{III}OH]$ and the Al(III) porphyrin components of H_2–Al and H_2–Al_2 were conveniently monitored at 600 nm. Fluorescence life times of H_2L^1, $[(L^1)Al^{III}OH]$, H_2–Al and H_2–Al_2 measured in toluene are summarized in Table 5. As seen from the data given in this table, the decays monitored at 600 nm for H_2–Al and H_2–Al_2 each showed an additional quenched component in comparison with the decay of $[(L^1)Al^{III}OH]$. Decays monitored at 720 nm of these arrays also showed a quenched component but both the extent of lifetime quenching and percentage contribution of this component were low. Overall, the time-resolved results corroborate the steady state results in that the values of %Q(Al) are higher than the corresponding %$Q(H_2)$.

We deduce, based on the steady-state and time-resolved fluorescence data, that quenching of the Al(III) porphyrin components in these donor-acceptor (D-A) systems is predominantly due to electronic energy transfer (EET) from the Al(III) porphyrin to the free base porphyrin. This EET is a thermodynamically favourable process in both H_2–Al and H_2–Al_2 [the singlet states of Al(III) and free base porphyrins are at 2.13 and 1.94 eV, respectively] as is the case with the P(V), Sn(IV) and Ge(IV) porphyrin based arrays investigated by us earlier. Indeed, as seen in Fig. 5, fluorescence spectra of both H_2–Al and H_2–Al_2 prominently show bands due to the free base component (*i.e.*, bands II and III) when excited at 550 nm. In addition, the excitation spectra of H_2–Al and H_2–Al_2 showed bands due to the Al(III) porphyrin when the emission was collected at 720 nm, where the emission is exclusively due to the free base component of these bichromophoric systems. Overlap of the corrected and normalized excitation spectra with the corresponding absorption spectra revealed that the EET efficiency is 80 ± 7% and 60 ± 7% for H_2–Al and H_2–Al_2, respectively, in toluene (see insets in Fig. 5). These EET efficiencies compare well with the corresponding %Q(Al) values (see Table 4). Thus, it appears that the quenching of fluorescence due to the Al(III) porphyrin components of these arrays is almost exclusively due to an EET process, although contribution from a photoinduced electron transfer (PET) from the singlet Al(III) porphyrin to the free base (the ΔG_{PET} values are −0.06 and −0.10 eV for H_2–Al and H_2–Al_2, respectively) cannot be neglected altogether in high polarity solvents.

Interestingly, the %$Q(H_2)$ values listed in Table 4 are lower than not only the %Q(Al) values but also the corresponding %$Q(H_2)$ values observed for the P(V) (93%), Sn(IV) (82%)and Ge(IV) (69%) porphyrin based trimers.[41,42] In these latter arrays, the strong quenching of their free base components has been attributed to a PET process from the singlet free base porphyrin to the ground state metalloid porphyrin. The free energy changes (ΔG_{PET}) associated with this process are

Table 4 Fluorescence data of H_2–Al, H_2–Al_2 and their monomeric analogues in various solvents[a]

	λ_{em}/nm (φ, %Q)							
	Toluene		CH_2Cl_2		CH_3CN		DMF	
Compound	λ_{ex} = 550 nm	λ_{ex} = 650 nm	λ_{ex} = 550 nm	λ_{ex} = 650 nm	λ_{ex} = 550 nm	λ_{ex} = 650 nm	λ_{ex} = 550 nm	λ_{ex} = 650 nm
H_2L^1	–	721 (0.14)	–	719 (0.11)	–	717 (0.09)	–	718 (0.14)
$[(L^1)Al^{III}OH]$	597, 647 (0.049)	–	601, 647 (0.059)	–	606, 660 (0.11)	–	608, 663 (0.087)	–
H_2–Al	599, 657, 723 (0.008, 84)	721 (0.13, 7)	601, 656, 721 (0.013, 78)	721 (0.10, 9)	607, 655, 720 (0.023, 79)	719 (0.07, 16)	608, 660, 722 (0.031, 65)	721 (0.12, 14)
H_2–Al_2	595, 663, 727 (0.016, 67)	727 (0.11, 21)	599, 658, 725 (0.033, 45)	725 (0.07, 36)	606, 665, 726 (0.060, 45)	726 (0.05, 44)	609, 675, 732 (0.038, 56)	733 (0.09, 35)

[a] Error limits: λ, ±1 nm; φ, ±10%.

Table 5 Fluorescence lifetime data of H_2L^1, $[(L^1)Al^{III}OH]$, H_2–Al, and H_2–Al_2 in toluene

Compound	λ_{ex}/nm	τ/ns (%A)	Ψ^2
H_2L^1	720	9.40 (100)	1.06
$[(L^1)Al^{III}OH]$	600	6.70 (73); 2.06 (27)	1.11
H_2–Al	600	6.80 (35); 2.11 (18); 0.17 (47)	1.06
	720	9.02 (84); 1.29 (16)	0.98
H_2–Al_2	600	6.64 (61); 2.20 (15); 0.26 (24)	1.08
	720	8.30 (68); 1.45 (32)	1.10

−0.45, −0.01 and 0.07 eV for the P(v), Sn(iv) and Ge(iv) analogues, respectively. The corresponding ΔG_{PET} values in CH_2Cl_2 for H_2–Al and H_2–Al_2 are estimated to be 0.22 and 0.25 eV, respectively. Interestingly, the exoergicity of these PET reactions follows a trend, *viz.* P(v) $\gg$ Sn(iv) > Ge(iv) > Al(iii), that is dependent on the electropositivity of the resident metalloid ion in the arrays, and it is consistent with the magnitudes of the corresponding %Q(H_2) values. We thus conclude that a photoinduced electron transfer from the singlet free base porphyrin to the Al(iii) porphyrin is weak in both H_2–Al and H_2–Al_2 but can, in principle, explain the low %Q(H_2) values observed for H_2–Al and H_2–Al_2. The observed general decrease of the ϕ values [or the increase in the %Q(H_2) values, see Table 4] with increasing polarity of the solvent is consistent with the participation of a charge transfer state in the excited state deactivation of the free base components of these systems.[47] However, an additional pathway for quenching that involves the heavy atom effect due to the presence of Al(iii) cannot be neglected altogether.

Inspection of the data given in Tables 4 and 5 additionally reveals that, in general, the %Q(Al) (which is due to EET) values are lower and the %Q(H_2) (which is due to PET) values are higher for the trimeric species in comparison with the corresponding dimer. A simplistic analysis indicates that the dimer is a bicomponent D-A system in which the donor/acceptor ratio is 1:1 for both EET and PET. On the other hand, the trimeric system has two donors [*i.e.*, Al(iii) porphyrins] and only one acceptor (*i.e.*, free base porphyrin) for EET and one donor (*i.e.*, free base porphyrin) and two acceptors [*i.e.*, Al(iii) porphyrins] for PET. This situation might rationalize the lower %Q(Al) and higher %Q(H_2) values observed for H_2–Al_2. Such a dependence of the quenching efficiency on the number of acceptor/donor subunits in a given D-A complex has been only suggested earlier in porphyrin arrays.[48]

In summary, new 'vertically-linked' dimeric and trimeric species based on the Al(iii) porphyrin scaffold have been synthesized and investigated by spectroscopic and electrochemical methods. Their photophysical properties have also been investigated and the results are interpreted in terms of intramolecular electron and energy transfer mechanisms. Noticeable differences exist in the properties of the dimers and trimers. Differences have also been noticed between the properties of the presently investigated trimers and the ones based on the P(v), Sn(iv) and Ge(iv) porphyrins studied by us earlier. These differences seem to arise not only from the differences in the electropositivity of the main group element ions bound to the porphyrin but also from the different topological features of these 'axial-bonding' type systems.

Acknowledgements

Financial support received from the BRNS (Mumbai, India) is gratefully acknowledged. In addition, we thank Professor J. K. M. Sanders and Dr. Nick Bampos (Cambridge, U. K.) for help with the 500 MHz NMR spectra and Professor N. Periasamy and A. S. R. Koti (TIFR, Mumbai, India) for the TCSPC measurements. PPK is thankful to the UGC for a senior research fellow award.

References

1 N. Aratani, A. Osuka, H. S. Cho and D. Kim, *J. Photochem. Photobiol., C*, 2002, **21**, 1.
2 D. Holten, D. F. Bocian and J. S. Lindsey, *Acc. Chem. Res.*, 2002, **35**, 57.
3 G. Simonneaux and P. L. Maux, *Coord. Chem. Rev.*, 2002, **228**, 43.
4 A. K. Burrell, D. L. Officer, P. G. Plieger and D. C. W. Reid, *Chem. Rev.*, 2001, **101**, 2751.
5 T. Imamura and K. Fukushima, *Coord. Chem. Rev.*, 2000, **198**, 133.
6 H. L. Anderson, *Chem. Commun.*, 1999, 2323.
7 D. Gust and T. A. Moore, in *The Porphyrin Handbook*, eds. K. M. Kadish, K. M. Smith and R. Guilard, Academic Press, London, 2000, vol. 8, pp. 153–167.
8 M.-S. Choi, T. Aida, T. Yamazaki and I. Yamazaki, *Chem.-Eur. J.*, 2002, **8**, 2667.
9 K. Sugou, K. Sasaki, T. Iwaki and Y. Kuroda, *J. Am. Chem. Soc.*, 2002, **124**, 1182.
10 E. Iengo, E. Zangrando, R. Minatel and E. Alessio, *J. Am. Chem. Soc.*, 2002, **124**, 1003.
11 M. Ayabe, A. Ikeda, Y. Kobo, M. Takeuchi and S. Shinkai, *Angew. Chem., Int. Ed.*, 2002, **41**, 2790.
12 M. L. Merlau, M. P. Mejia, S. B. T. Nguyen and J. T. Hupp, *Angew. Chem., Int. Ed.*, 2001, **40**, 4239.
13 J. Wojaczynski and L. Latos-Grazynski, *Coord. Chem. Rev.*, 2000, **204**, 113.
14 J. K. M. Sanders, N. Bampos, Z. Clyde-Watson, S. L. Darling, J. C. Hawley, H.-J. Kim, C. C. Mak and S. J. Webb, in *The Porphyrin Handbook*, eds. K. M. Kadish, K. M. Smith and R. Guilard, Academic Press, London, 2000, vol. 3, pp. 1–48.
15 K. Susumu, K. Tanaka, T. Shimidzu, Y. Takeuchi and H. Segawa, *J. Chem. Soc., Perkin. Trans. 2*, 1999, 1521.
16 H. Segawa, K. Kunimoto, K. Susumu, M. Taniguchi and T. Shimidzu, *J. Am. Chem. Soc.*, 1994, **116**, 11 193.
17 K. Susumu, K. Kunimoto, H. Segawa and T. Shimidzu, *J. Phys. Chem.*, 1995, **99**, 29.
18 G. D. Fallon, S. J. Langford, M. A.-P. Lee and E. Lygris, *Inorg. Chem. Commun.*, 2002, **5**, 715.
19 J. E. Redmann, N. Feeder, S. J. Teat and J. K. M. Sanders, *Inorg. Chem.*, 2001, **40**, 2486.
20 J. Wojaczynski, L. Latos-Grazynski, M. M. Olmstead and A. L. Balch, *Inorg. Chem.*, 1997, **36**, 4548.
21 J. Wojaczynski and L. Latos-Grazynski, *Inorg. Chem.*, 1995, **34**, 1054.
22 D. F. Shriver, P. W. Atkins and C. H. Langford, *Inorganic Chemistry*, Oxford University Press, Oxford, 1990, p. 332.
23 T. Aida, H. Sugimoto, M. Kuroki and S. Inoue, *J. Phys. Org. Chem.*, 1995, **8**, 249.
24 M. Komatsu and T. Aida, *J. Am. Chem. Soc.*, 1991, **113**, 8492.
25 Y. Sato, T. Arai and S. Inoue, *Chem. Lett.*, 1990, **4**, 551.
26 K. Konishi, T. Aida and S. Inoue, *J. Org. Chem.*, 1990, **55**, 816.
27 K. Konishi, K. Makita, T. Aida and S. Inoue, *J. Chem. Soc., Chem. Commun.*, 1988, 643.
28 D. D. Perrin, W. L. F. Armarego and D. R. Perrin, *Purification of Laboratory Chemicals*, Pergamon, Oxford, 1986.
29 J. S. Lindsey, I. C. Schreiman, H. C. Hsu, P. C. Kearney and A. M. Marguerettaz, *J. Org. Chem.*, 1987, **52**, 827.
30 R. G. Little, *J. Heterocycl. Chem.*, 1978, **15**, 203.
31 C.-H. Lee and J. S. Lindsey, *Tetrahedron*, 1994, **50**, 11 427.
32 Y. Kaizu, N. Misu, K. Tsuji, Y. Kaneko and H. Kobayashi, *Bull. Chem. Soc. Jpn.*, 1985, **58**, 103.
33 J.-H. Fuhrhop and K. M. Smith, in *Porphyrins and Metalloporphyrins*, ed. K. M. Smith, Elsevier, Amsterdam, 1975, p. 978.
34 D. J. Quimby and F. R. Longo, *J. Am. Chem. Soc.*, 1975, **19**, 5111.
35 A. Harriman and J. Davila, *Tetrahedron*, 1989, **45**, 4737.
36 L. Giribabu, A. A. Kumar, V. Neeraja and B. G. Maiya, *Angew. Chem., Int. Ed.*, 2001, **40**, 3621.
37 M. Sirish, R. Kache and B. G. Maiya, *J. Photochem. Photobiol., A*, 1996, **93**, 129.
38 M. Sirish and B. G. Maiya, *J. Photochem. Photobiol., A*, 1995, **88**, 127.
39 B. G. Maiya, S. Doraisamy, N. Periasamy and B. Venkataraman, *J. Photochem. Photobiol., A*, 1994, **81**, 139.
40 M. Sirish and B. G. Maiya, *J. Photochem. Photobiol., A*, 1994, **77**, 189.

41 T. A. Rao and B. G. Maiya, *J. Chem. Soc., Chem. Commun.*, 1995, 939.

42 L. Giribabu, T. A. Rao and B. G. Maiya, *Inorg. Chem.*, 1999, **38**, 4971.

43 A. A. Kumar, L. Giribabu, D. R. Reddy and B. G. Maiya, *Inorg. Chem.*, 2001, **40**, 6757.

44 B. G. Maiya, N. Bampos, A. A. Kumar, N. Feeder and J. K. M. Sanders, *New J. Chem.*, 2001, **25**, 797.

45 D. R. Reddy and B. G. Maiya, *J. Porphyrins Phthalocyanines*, 2002, **6**, 3.

46 R. J. Abraham, G. R. Bedford, D. McNeillie and B. Wright, *Org. Magn. Reson.*, 1980, **14**, 418.

47 P. Suppan, *Chimia*, 1988, **42**, 320.

48 D. Kuciauskas, P. A. Liddell, S. Lin, T. E. Johnson, S. J. Weghorn, J. S. Lindsey, A. L. Moore, T. A. Moore and D. Gust, *J. Am. Chem. Soc.*, 1999, **121**, 8604.